International Journal of Engineering Research & Technology (IJERT)
ISSN: 2278-0181
Vol. 4 Issue 07, July-2015

Analysis of Straight Bladed Vertical Axis Wind Turbine

H. E. Saber
Teaching Assistant.
Department of Mechanical Engineering
Arab Academy for Science Technology & Maritime Transport
Alexandria –Egypt

E. M. Attia
Associate Prof
Department of Mechanical Engineering
Arab Academy for Science Technology & Maritime Transport
Alexandria –Egypt

H. A. El Gamal
Professor
Department of Mechanical Engineering
Alexandria University
Alexandria –Egypt

Abstract: **This work analyses the link between the geometry of a vertical-axis straight-bladed wind turbine and its performance (power coefficient). The geometry of a vertical-axis wind turbine cause Reynolds number variations. Any changes in the power coefficient which can also be studied to derive how its variation affect turbine performance. Using a calculation code based on the Double Multiple Stream Tube , symmetrical straight-bladed wind turbine performance was evaluated as for various solidity . This numerical analysis highlighted how turbine performance is strongly influenced by the Reynolds number of the rotor blade. Also A dimensional analysis is introduced and is to be considered to generalize the design for different turbine specifications. One of the qualities of dimensional analysis is that geometrically similar turbines will produce the same non-dimensional results. This allows one to make comparison between different size wind turbines in terms of power output and other related variables**.

Keywords: Vertical axis Wind turbine – Straight bladed wind turbine – Darrieus Wind turbine – Analysis of Wind turbines

I. INTRODUCTION

Paraschivoiu et. al [1] presented an optimal computation of blade's pitch angle of an H-D Darrieus wind turbine to obtain maximum torque; with some results presented using a 7 kW prototype. In order to determine the performances of the straight bladed vertical axis wind turbine a genetic algorithm optimizer is applied in addition to an improved version of "Double Multiple stream tube" model. Where in this model a partition of the rotor is considered in the stream tubes and treats each of the two blade elements defined by a given stream tube as an actuator disk. Dominy et.al [2] in his presentation of vertical axis wind turbines explained the potential advantages of using Darrieus type wind turbines in the small scale and domestic applications where the cost , reliability are very important points in addition to the simplicity of design structure, generator and control system. His concern was about the ability of the Darrieus turbines to be self-started. Olson and Visser [3] showed the availability of using Darrieus turbines in commercial grid connected utility scale operations. Also, he mentioned the development of marketing small scale wind turbines due to the social "going green" phenomena and to its economic stand point. Batista et. al [4] mentioned the great interest in the vertical axis wind turbine due to the rapid increase in its power generation, and the need for a smarter electrical grid with a decentralized energy generation, especially in the urban areas. However, estimation of the performance of Darrieus type VAWT is very tough as the blades rotate in three dimension space around the rotor which results in several flow phenomena such as dynamic stall, flow separation, flow wake and natural incapability to self-starting. Klimas[5] described Darrieus turbines as relatively simple machines. Since, they have fixed blade geometry, usually two or three blades rotate about a vertical axis rotor generating power to a ground mounted power conversion or absorption machinery, with no yaw control nor power regulation . Nila et al. [6] dealt with the calculations of a fixed-pitch straight-bladed vertical axis wind turbine of the 'Darrieus Type'. They made a case study using a well-known NACA0012 turbine blade

profile where the wind load calculations were achieved by assuming solid frontal areas of the blades and tower instruction; also he assumed that each section of a blade behaves as an airfoil in a two dimensional flow field to analyze the Darrieus rotor in an elementary way Lobitz [7] showed the importance of the dynamic response characteristics of the VAWT rotor and its influence in the safety and fatigue life of VAWT systems.He also mentioned that the problem is to predict the critical speed "resonance" and the forced vibration response amplitude.

Sabaeifardet.al [8] discussed the potential of using VAWT at buildings. As, they do not suffer from changing wind direction, simplicity of design specially when they are integrated with building architecture, and they have a better response when they face a turbulence flow especially in urban areas. He explained the aerodynamics and the performance of small scale Darrieus type straight-bladed VAWT through a computational and an experimental study. Also, he mentioned some design parameters that could affect the performance such as number of blades, aerofoil type and turbine solidity. Cristia [9] presented a study about urban wind turbines and their ability to be used near populated areas. Cristia mentioned in his study different technical and design solutions, advantages and disadvantages, also the problems affecting these wind turbines such as noise and shadows. Many design methods was introduced to achieve various possible solutions where a comparison can be made to conclude the most suitable solutions. Kishore [10] focused his study on using small scale wind turbines used at ground level and low wind speed. The aim of the study was to provide a systematic design and development of this turbine. In his study he used an inverse design and optimization tool based on Blade Element Momentum theory.

Rathi [11] presented the advantages of VAWT over HAWT for small scale or residential use.. In order to predict the power generations by an H-Type Darrieus wind turbine with varying pitch blades, a Double-Multiple stream tube model is used with some modifications. Also, a dynamic model was devised and analyzed. Hall [12] showed that the kinetic energy of water currents can be used as a source of energy production. He also presented the advantages of using a cross flow hydrokinetic turbine (CFHT) over a normal horizontal axis wind turbine in the context of energy harvesting; such as independence from current direction, reversibility, stacking and self-starting without complex pitch mechanism. He focused his study on the flow past a CFHT and the hydrodynamic forces created by the flow on the blades.

Castillo [13] introduced a new design of small vertical axis wind turbine rotor using solid wood as a construction material. In Castillo's work the aerodynamic analysis were made by a momentum based model with the aid of a mathematical computer program MATLAB. After evaluating the effect of several parameters on turbine efficiency, torque and acceleration, a prototype test was introduced for three bladed wind turbine models.

Milgliore, Fritschen and Mitchel [14] introduced in their work the importance of choosing the aerofoil blade shape and its effect on improving the aerodynamic performance for a Darrieus wind turbine blade. The analysis was made under some specifications as using two bladed machine with an infinite aspect ratio, rotor solidity from 7 to 21 percent and operating at Reynolds number nearly to three million.

Reddy [15] aimed to analyze and predict the performance of the Darrieus wind turbine. The analysis was carried out by using the multiple stream tube concept. In addition to using the standard blade element theory to compute the induced flow velocity which is going to be used in predicting the force on each rotor blade element. A computer model DART was constructed that can predict the rotor performance with reasonable accuracy; as it can also shows the effects of rotor geometry on such blade solidity and height to diameter ratios.

Scheurich [16] showed interest in using vertical axis wind turbines VAWT in urban areas. He mentioned also the difficulty to compute an accurate modeling of the aerodynamics, due to the unsteadiness in their aerodynamic loading, as the cyclic motion of the turbine varies the angle of attack for each rotor revolution.

II. THEORITICAL ANALYSIS

In this section the simulation model isassumed to be the Double Multiple Stream Tube (DMST) Model. This model is a combination between the MST model and double actuator theory [17], where the turbine is modeled separately for the upstream half and the downstream half. Also an assumption is made that the wake from the upwind pass is fully expanded and the ultimate wake velocity has been reached before the interaction with the blades in the downwind pass.

Fig. 1 presents the DMST model diagram. Each airfoil in the DMST model intersects each stream tube twice, one on the upwind pass and the other on the downwind pass. The DMST model solves two equations simultaneously for the stream-wise force at the actuator disk; one obtained by conversation of momentum and other based on the aerodynamic coefficients of the airfoil (Lift and Drag) and the local wind velocity. These equations are solved twice, one for the upwind part and another for the downwind part.

A- Upwind Un-pitched Blade Analysis:

The velocity components on an upwind blade section are illustrated by Fig. 2 the analysis of these components can be obtained as the following.

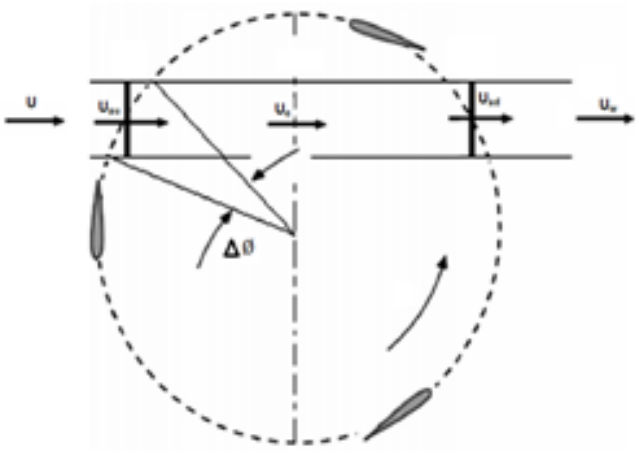

Fig.. 1: Plan view of a double-multiple-stream tube analysis of the flow through a VAWT rotor.

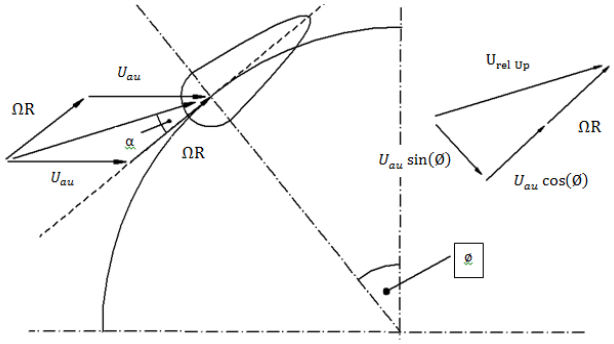

Fig. .2: Velocity components acting on an upwind blade element.

The local resultant velocity is:

$$U_{rel\ Up}^2 = [\Omega R + (1 - a_u)U\cos(\emptyset)]^2 + [(1 - a_u)U\sin(\emptyset)]^2 \quad (1)$$

$$\frac{U_{rel\ Up}}{U} = \sqrt{\begin{matrix}[(\lambda + (1 - a_u)\cos(\emptyset)]^2 \\ + [(1 - a_u)\sin(\emptyset)]^2\end{matrix}} \quad (2)$$

And local angle of attack is represented by:

$$\alpha = \tan^{-1}\frac{[(1-a_u)\sin(\emptyset)]}{[\lambda+(1-a_u)\cos(\emptyset)]} \quad (3)$$

Fig.3 shows the force coefficient analysis diagram, on an upwind blade section, where:

$$\emptyset_L = \tan^{-1}\frac{CD}{CL} \quad (4)$$

Normal force Coefficient:

$$C_N = C_D\sin(\alpha) + C_L\cos(\alpha) \quad (5)$$

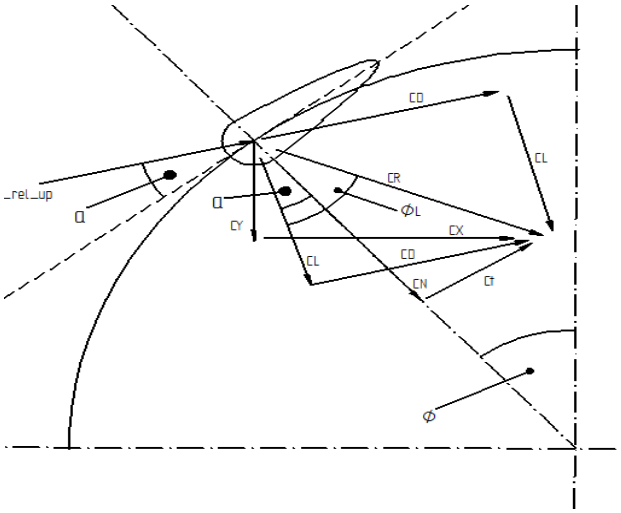

Fig.3: force analysis diagram on an upwind blade element

Tangential force Coefficient:

$$C_t = -C_L\sin(\alpha) + C_D\cos(\alpha) \quad (6)$$

The force coefficients in *x* and *y* directions can be expressed as:

$$C_x = C_N\sin(\emptyset) + C_t\cos(\emptyset) \quad (7)$$

$$C_y = C_N\cos(\emptyset) - C_t\sin(\emptyset) \quad (8)$$

Thrust force Coefficient:

$$C_{FT} = C_t\cos(\emptyset) + C_N\sin(\emptyset) \quad (9)$$

Upwind average aerodynamic thrust can be expressed by a non-dimensional thrust coefficient as follows:

$$C_{FT} = \frac{N\sum_{i=1}^{m}\frac{1}{2}\rho U_{rel\ up}^2(hc)(C_t\cos(\emptyset) - C_N\sin(\emptyset))\frac{\Delta(\emptyset)}{2\pi}}{\frac{1}{2}\rho U^2(hR)(m)\Delta(\emptyset)\sin(\emptyset)} \quad (10)$$

Where m is the number of stream tubes used.

The instantaneous torque can be expressed by:

$$Q_i = \frac{1}{2}\rho U_{rel}^2(hc)\,C_tR \quad (11)$$

The average torque:

$$Q_a = N\frac{\sum_{i=1}^{i=m}\frac{1}{2}\rho U_{rel}^2(hc)C_tR}{m} \quad (12)$$

The torque coefficient can be expressed as:

$$C_Q = \frac{Q_a}{\frac{1}{2}\rho U^2 (Dh)R} = \left(\frac{Nc}{D}\right) \sum_{i=1}^{m} \frac{\left(\frac{U_{rel}}{U}\right)^2 C_t}{m} \quad (13)$$

The Power coefficient can be expressed as:

$$C_P = C_Q \lambda \quad (14)$$

B. Downwind Un-pitched Blade Analysis:

The velocity components for the downwind part can be demonstrated by Fig. 4 and the Equation of velocity components in the downwind section.

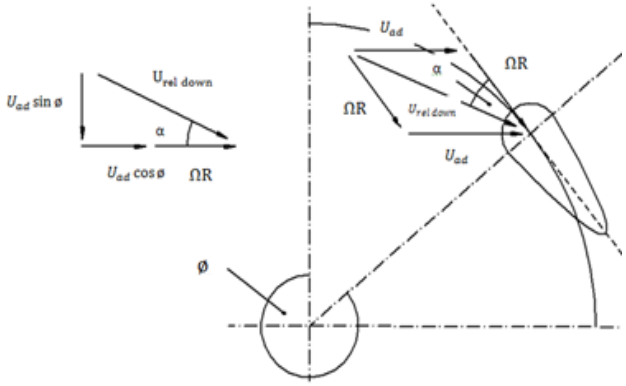

Fig.4: velocity components acting on a downwind blade element.

Where local resultant velocity is:

$$U_{rel\ down}^2 = [\Omega R + U(1-2a_u)(1-a_d)\cos(Ø)]^2 + [-(1-a_d)(1-2a_u)U\sin(Ø)]^2 \quad (15)$$

$$\frac{U_{rel\ down}}{U} = \sqrt{\begin{matrix}[(\lambda + (1-2a_u)(1-a_d)\cos(Ø)]^2 \\ + [-(1-2a_u)(1-a_d)\sin(Ø)]^2\end{matrix}} \quad (16)$$

And local angle of attack:

$$\boldsymbol{\alpha = \tan^{-1} \frac{-[(1-2a_u)(1-a_d)\sin(Ø)]}{[\lambda+(1-2a_u)(1-a_d)\cos(Ø)]}} \quad \textbf{(17)}$$

Fig.5Shows the force coefficient analysis diagram, on a downwind blade section, where:

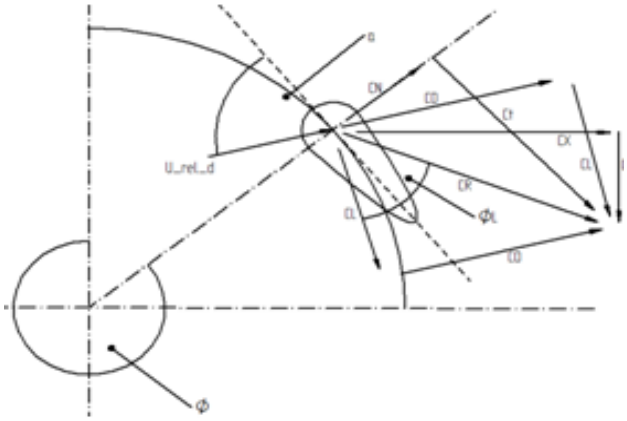

Fig.5: force analysis diagram of a downwind blade element

$$Ø_L = \tan^{-1} \frac{CD}{CL} \quad (18)$$

Normal force Coefficient:

$$C_N = -C_L \cos(\alpha) + C_D \sin(\alpha) \quad (19)$$

Tangential force Coefficient:

$$C_t = C_D \cos(\alpha) + C_L \sin(\alpha) \quad (20)$$

The force coefficients in *x* and *y* directions can be expressed as:

$$C_x = -C_N \sin(Ø) + C_t \cos(Ø) \quad (21)$$

$$C_y = -C_N \cos(Ø) - C_t \sin(Ø) \quad (22)$$

Thrust force Coefficient:

$$C_{FT} = C_t \cos(Ø) - C_N \sin(Ø) \quad (23)$$

Downwind average aerodynamic thrust can be represented in a non-dimensional thrust coefficient as follows:

$$C_{FT} = \frac{N \sum_{i=1}^{m} \frac{1}{2}\rho U_{rel\ down}^2 (hc)(C_t \cos(Ø) - C_N \sin(Ø)) \frac{\Delta(Ø)}{2\pi}}{\frac{1}{2}\rho U_e^2 (hR)(m)\Delta(Ø)\sin(Ø)} \quad (24)$$

Instantaneous torque:

$$Q_i = \frac{1}{2}(U_{rel\ down})^2 (hc) C_t R \quad (25)$$

Average torque:

$$Q_a = N \frac{\sum_{i=1}^{i=m} \frac{1}{2}\rho U_{rel\ down}^2 (hc) C_t R}{m} \quad (26)$$

The torque coefficient can be expressed as:

$$C_Q = \frac{Q_a}{\frac{1}{2}\rho U_e^2 (Dh)R} = \left(\frac{Nc}{D}\right) \sum_{i=1}^{m} \frac{\left(\frac{U_{rel\ down}}{U_e}\right)^2 Ct}{m} \quad (27)$$

The Power coefficient can be expressed as:

$$C_P = C_Q \lambda \quad (28)$$

III. GENENARL SOLUTION

The angle of attack α and $\Delta\emptyset$ plays a big rule in the forces coefficient direction and magnitude. However, we can illustrate a general solution as shown in Fig.6, where the angle of attack is the only parameter changing the forces coefficient magnitude and direction, as shown below:

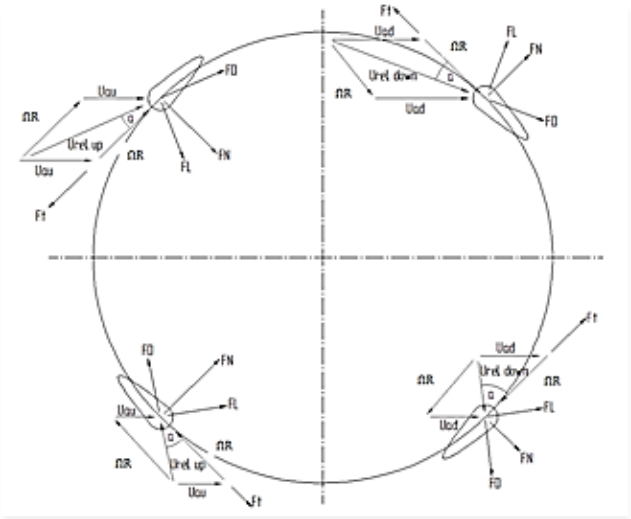

Fig..6: General solution Forces and velocity triangle .

For upwind section the relative upwind velocity is:

$$\frac{U_{rel\ Up}}{U} = \sqrt{[(\lambda + (1 - a_u)\cos(\emptyset)]^2 + [(1 - a_u)\sin(\emptyset)]^2} \quad (29)$$

If the angle of attack is below 90 degrees, then:

$$C_N = C_L \cos(\alpha) + C_D \sin(\alpha) \quad (30)$$

$$C_t = -C_D \cos(\alpha) + C_L \sin(\alpha) \quad (31)$$

$$C_x = -C_N \sin(\emptyset) + C_t \cos(\emptyset) \quad (32)$$

$$C_y = -C_N \cos(\emptyset) - C_t \sin(\emptyset) \quad (33)$$

$$C_{FT} = -C_t \frac{\cos\emptyset}{\sin\emptyset} + C_N \quad (34)$$

If the angle of attack is greater than 90 degrees, then:

$$C_N = -C_L \cos(\alpha) + C_D \sin(\alpha) \quad (35)$$

$$C_t = -C_D \cos(\alpha) - C_L \sin(\alpha) \quad (36)$$

$$C_x = -C_N \sin(\emptyset) + C_t \cos(\emptyset) \quad (37)$$

$$C_y = -C_N \cos(\emptyset) - C_t \sin(\emptyset) \quad (38)$$

$$C_{FT} = -C_t \frac{\cos\emptyset}{\sin\emptyset} + C_N \quad (39)$$

While for downwind section the relative downwind velocity:

$$\frac{U_{rel\ down}}{U} = \sqrt{\begin{matrix}[(\lambda + (1 - 2a_u)(1 - a_d)\cos(\emptyset)]^2 \\ + [-(1 - 2a_u)(1 - a_d)\sin(\emptyset)]^2\end{matrix}} \quad (40)$$

If the angle of attack is below 90 degrees, then:

$$C_N = C_L \cos(\alpha) + C_D \sin(\alpha) \quad (41)$$

$$C_t = -C_D \cos(\alpha) + C_L \sin(\alpha) \quad (42)$$

$$C_x = C_N \sin(\emptyset) + C_t \cos(\emptyset) \quad (43)$$

$$C_y = C_N \cos(\emptyset) - C_t \sin(\emptyset) \quad (44)$$

$$C_{FT} = C_t \frac{\cos\emptyset}{\sin\emptyset} + C_N \quad (45)$$

If the angle of attack is greater than 90 degrees, then:

$$C_N = -C_L \cos(\alpha) + C_D \sin(\alpha) \quad (46)$$

$$C_t = -C_D \cos(\alpha) - C_L \sin(\alpha) \quad (47)$$

$$C_x = C_N \sin(\emptyset) + C_t \cos(\emptyset) \quad (48)$$

$$C_y = C_N \cos(\emptyset) - C_t \sin(\emptyset) \quad (49)$$

$$C_{FT} = C_t \frac{\cos\emptyset}{\sin\emptyset} + C_N \quad (50)$$

IV. COMPUTATIONAL PROCEDURE

The computational procedure for a given rotor geometry and rotational speed are done through several steps. The first one is obtaining the relative wind velocity acting on a blade. Secondly, is the blade section lift and drag coefficients; both coefficients are obtained through known experimental data of Sheldal and Klimas[18] using the local blade section Reynolds number and the local angle of attack, the selection of this coefficient through the mentioned parameters are done with the aid of a "MATLAB" tooling box called "SFTOOL". Where Reynolds number can be expressed as:

$$R_{eb} = \frac{\rho U_{rel} C}{\mu_\infty} \quad (51)$$

As μ_∞ is the dynamic viscosity, C is the chord length. In order to calculate the local Reynolds number, we need to obtain the relative velocity U_{rel} and to calculate the relative velocity; we make an initial guess for the axial induction factor, equal to

zero. The next step is calculating the normal and tangential force coefficients then, we calculate the thrust coefficient derived from aerodynamic forces and from the actuator disk theory. Compare between both thrust coefficients obtained from both theories. If the thrust coefficients are the same, then the convergence is achieved. If not then we change the axial induction factor and follow the same steps until the convergence is achieved. As the convergence is achieved per stream tube, we calculate the relative velocity, angle of attack, torque and power. Convergence may be rapid with a relative error less than10^{-2}. A similar procedure is adopted for the downwind half cycle. The induction factor is calculated twice for all stream tubes, one for the upwind half stream a_u and one for the downwind half stream a_d.

V. DIMENSIONAL ANALYSIS

Wind turbines come in different sizes. They experience a wide range of variables when in operation. These variables complicate the process of comparison of different size of turbines in terms of their performance. The general geometric features of H-rotors are rotor radius *R*, blade length h, number of blades *N*, chord length *C* and airfoil shape. These features are all determinants to the aerodynamic performance of the rotor. The environmental conditions include wind velocity U air viscosity μ, air density ρand also the angular rotating speed of the H-rotor Ω**.** Usually, the performance of an H-rotor is evaluated by the power coefficient defined as the ratio of the power that the turbine can extract from the wind energy. To deal with this, the help of dimensional analysis is required. One of the advantages of dimensional analysis is that geometrically similar turbines will produce the same non-dimensional results. This allows one to make comparison between different size wind turbines in terms of power output and other related variables. Based on the determinants of the rotor performance, the power coefficient $C_p$can be expressed as a function of rotational speed Ω, free stream wind velocity *U*, rotor radius *R*, blade length h, number of blades *N*, chord length *C*, fluid viscosity μ and fluid density ρ.There are nine parameters relevant to the power of wind turbine. The power can simply be expressed at

$$P = f\{U, \mu, \rho, R, C, h, N, \Omega\}. \quad (52)$$

According to Buckingham Pi-theorem, the functional relationship of the dimensionless groups may be obtained and the result may written as:

$$\frac{P}{\rho R^2 U^3} = f\left\{\frac{C}{R}, \frac{h}{R}, N, \frac{\Omega R}{U}, \frac{\mu}{U\rho R}\right\} \quad (53)$$

The solution may be correct but expressed in terms of Pi-groups which have no recognizable physical significance. It may then be necessary to combine the pi-groups to obtain new groups which have significance. A solidity term, free stream Reynolds number, power coefficient and tip speed ratio can be expressed as:

$$\text{solidity } \sigma = \frac{NC}{R}$$

$$\text{free stream reynolds number } Re_\infty = \frac{U \rho R}{\mu}$$

$$\text{Power Coefficient } C_P = \frac{P}{\rho R \ hU^3}$$

$$\text{Tip Speed Ratio } \lambda = \frac{\Omega R}{U}$$

By considering the new Pi-groups as mentioned above, the power coefficient C_P can be expressed as a function of tip speed ratio λ, free stream Reynolds number Re_∞ and solidity □.

$$C_P = f\{Re_\infty, \lambda, \sigma\} \quad (54)$$

VI. RESULTS AND DISCUSSION

The results obtained from the theoretical analysis explained presented and discussed. The presentation is to be divided into three main parts; the first one is about the detailed analyses, which includes the parameters affecting the turbine outputs as a function of the azimuthal angle and its effect on the turbine performance. The second one is about the dimensional analysis, where we can consider design charts that can be used for any proposed VAWT design under specific limitations.

A. Effect of Wind Speed on the Power Coefficient:

In this section the effect of different wind speeds (5,6,7,8,9,10 m/s) on the average power coefficient C_p, are discussed for a turbine of 0.2 meter chord length, three blades, 1 meter blade height, blade profile NACA0012 and 2 meter turbine radius as shown in Fig.7. Many features can be concluded from this figure; firstly, by increasing the wind speed the maximum average power coefficient increases. This takes place since, by increasing the wind speeds the torque extracted by the turbine increases leading to a higher power coefficient such as shown in Fig.8. The second feature, which needs to be explained, is the relationship between tip speed ratio λ and the power coefficientC_p. At low λ (below 3.5) C_p is mainly negative while at larger values of λ (above 3.5) is positive.

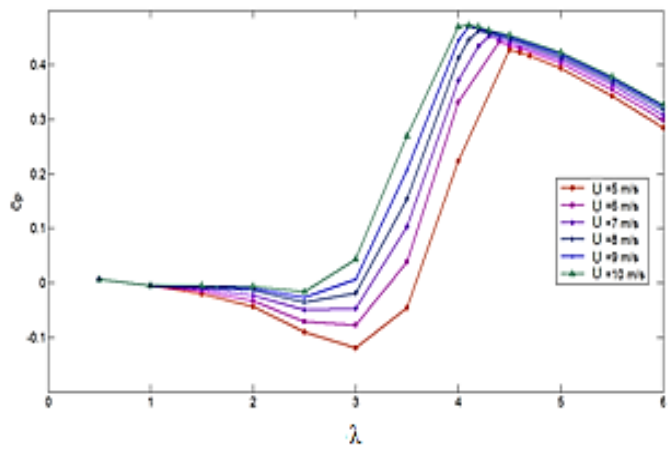

Fig.7 Relation between tip speed ratio λ and power coefficient Cp for different inlet wind speed

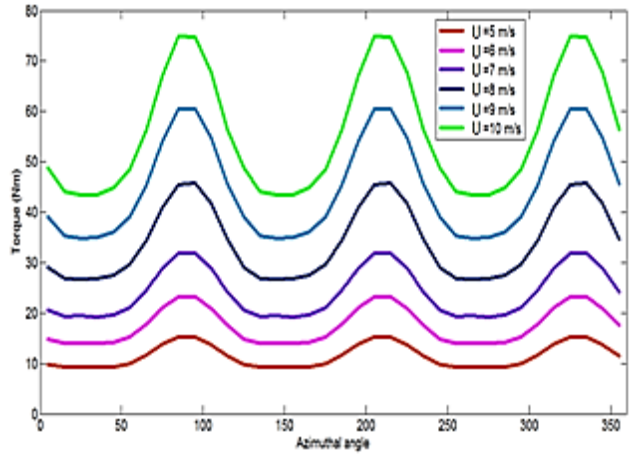

Fig. 8 Torque versus Azimuthal angle for different inlet wind speeds at maximum Cp

In order to explain this relation, we need to look at the turbine characteristics such as, torque, angle of attack, normal and tangential forces coefficient and relative velocity acting on the blade. The third region is the higher tip speed ratio region in which when the tip speed ratio increases beyond the design condition 4.5 (Maximum C_p). The power coefficient starts to decrease due to the decrease in the mean torque, while the turbine performance remains nearly the same with small change such as in tip speed ratio 5.5 and 6. In order to know why the mean torque changes at different tip speed ratios we have to look at the previous analysis. Where the tangential force coefficients and the blade relative velocities are the main parameters affecting the mean torque value. Those coefficients are functions of the lift and drag forces coefficients which are functions of the angle of attack and blade Reynolds number. It can thus According to Sheldal and Klimas[18] experimental data and equations of c_t; a relationship between the angle of attack, blade Reynolds number and tangential force coefficients can be found, and is shown in Fig. 9.

It can be seen in the previous figure, for all blade Reynolds number as we increase α above nearly 45° the tangential force coefficient is always positive especially in the region above 90°, while for α in the range of 25° to 45° the tangential force coefficients is mainly negative. On the other hand for α below 25° the tangential force coefficients sign depends on the blade Reynolds number specially at low blade Reynolds number (below $4x10^6$). So according to the case U=5m/s, Fig.10 gives a relationship between the blade's angle of attack, Reynolds number and tangential force coefficient with respect to the azimuthal angle at different tip speed ratios.

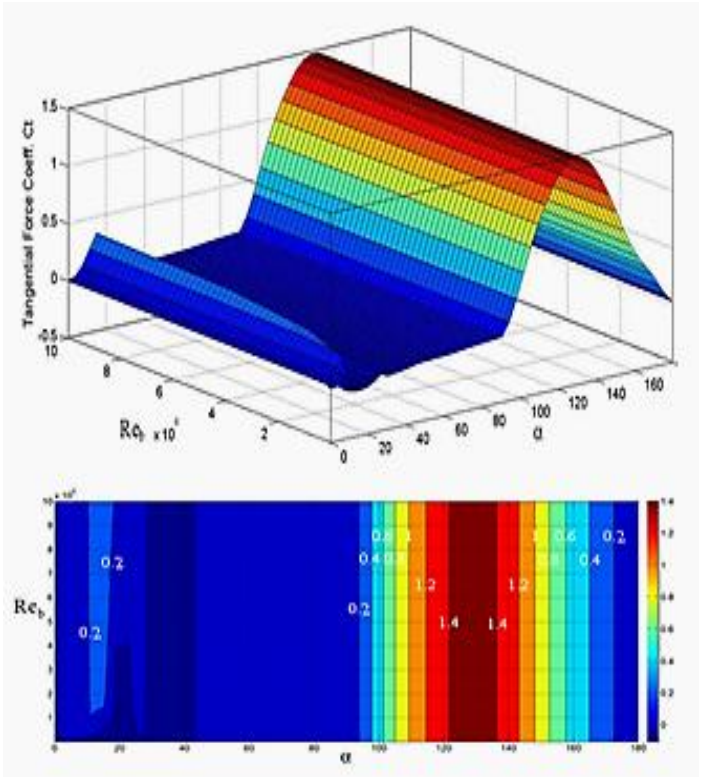

Fig.9 Relation between angle of attack (α), blade Reynolds number and Tangential force coefficient C_t

So from Fig.11) it is concluded that, as both angle of attack and blade Reynolds number changes during the hall rotation, the tangential force coefficient also changes. However figure (16) cannot describe the turbine performance curve in figure (14). As the power coefficient is found to be a function of the mean torque which is a function of both tangential force coefficient and blade's relative velocity squared.

B-Effect of Turbine geometry on the power coefficient:

The main turbine geometry parameters affecting the turbine output are the blade chord length, blade height, along with turbine radius. The effect of each parameter on the power coefficient is to be considered maintaining the turbine swept area constant equal to 16 m^2. The effects are to be examined for a three bladed turbine and for an airfoil shape

NACA0012. In this section the effect of different chord lengths on the power coefficient is presented for a turbine of 2 m blade height, 4 m turbine radius, inlet velocity of 5 m/s and swept area of 16 m^2.

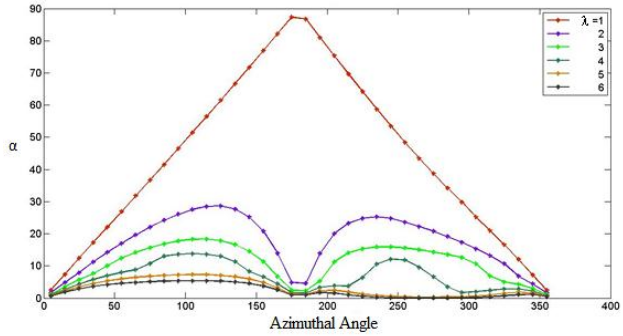

Case (a) a relation between angle of attack and Azimuthal angle at differenttip speed ratios

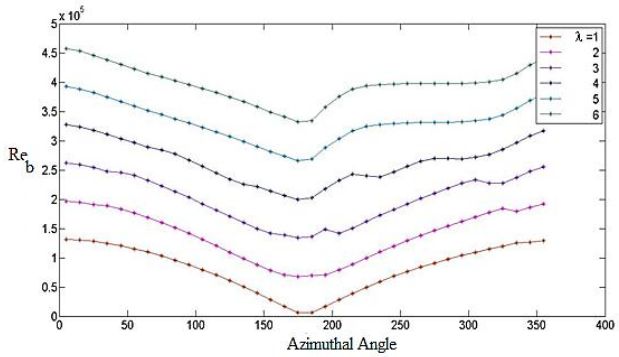

Case (b): a relation between blade's Reynolds number and Azimuthal angle at different tip speed ratios

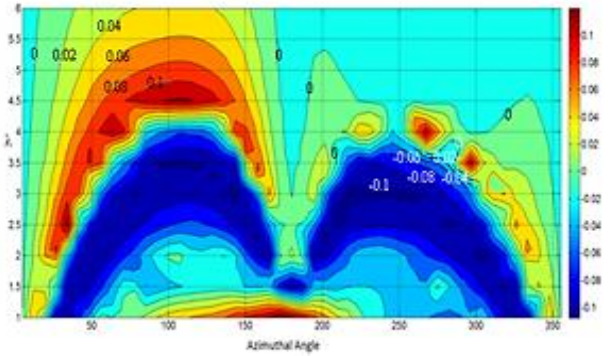

Case(c) a relation between Tangential force coefficient and Azimuthal angle at different tip speed ratios

Fig. 10 Relation between angle of attack, blade's Reynolds number and Tangential force coefficient Ct at different tip speed ratio

Figure (18), shows that when the chord length is increased the maximum average power coefficient increases. Also by increasing the chord length the negative average power coefficient at low tip speed ratio starts to decrease.

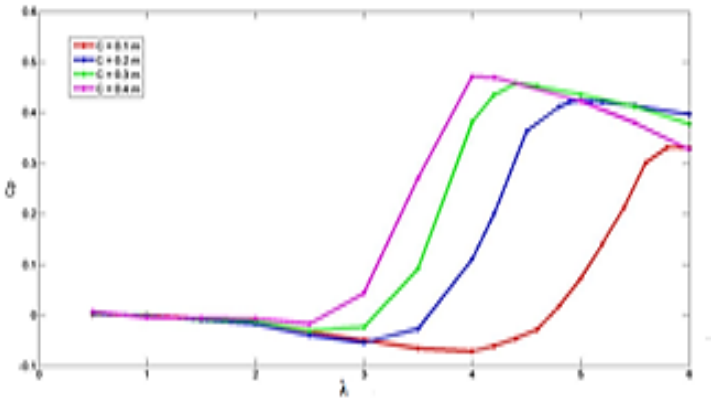

Fig.11 Effect of different turbine chord length C on the average power coefficient for different tip speed ratio λ

The effect of different turbine radius on the average power coefficient is considered her, for an inlet velocity of 5 m/s, chord length of 0.2 m and swept area of 16 m^2.

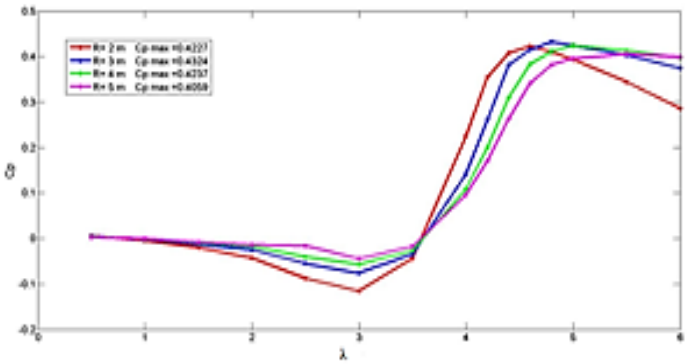

Fig.12 Effect turbine radius on the relation between the average power coefficient and the tip speed ratio λ

From Fig. 12, it can be seen that as we decrease the rotor radius the maximum power coefficient increases. But at rotor radius equal to 2m the power coefficient starts to increase. Also it is noticed that at low λ increasing the rotor radius will lead to a lower negative power coefficients. The results mentioned in the above sections are only applicable for those turbine characteristics mentioned in every section. So a dimensional analysis is to be considered to generalize the design for different turbine specifications.

C-Dimensional Analysis results:

The results presented in previous sections are only applicable for turbine characteristic considered in each section. A dimensional analysis is required and is to be considered to generalize the design for different turbine specifications. One of the qualities of dimensional analysis is that geometrically similar turbines will produce the same non-dimensional

results. This allows one to make comparison between different size wind turbines in terms of power output and other related variables. Based on the study of the dimensional analysis given in the previous chapter, the power coefficient C_P can be expressed as a function of tip speed ratio λ, free stream Reynolds number Re_∞ and solidity □.

$$C_P = f\{Re_\infty, \lambda, \sigma\}$$

From this relation design charts such as shown in Fig. 13 can be considered showing the relation between Power coefficient C_P, free stream Reynolds number Re_∞ and Tip speed ratio λ at specific Rotor solidities σ. A check was made for the power coefficient calculated by the dimensional analysis and that calculated by the main program. This comparison was done for different rotor solidities, free stream Reynolds number and tip speed ratios and complete agreement was found.

CONCLUSIONS

From the present work the following conclusions are drawn:

- The higher the wind speed the higher the maximum average power coefficient.
- The higher the wind speed the lower tip speed ratio corresponding to the maximum average power coefficient.
- The power coefficient is a function of three main parameters namely the free stream Reynolds number, tip speed ratio and rotor solidity.
- The higher the rotor solidity the higher the maximum average power coefficient with a decrease in the negative power coefficient at low tip speed ratio.
- As the tip speed ratio increases, reaching the maximum average power coefficient the torque fluctuation reaches nearly a sinusoidal wave.

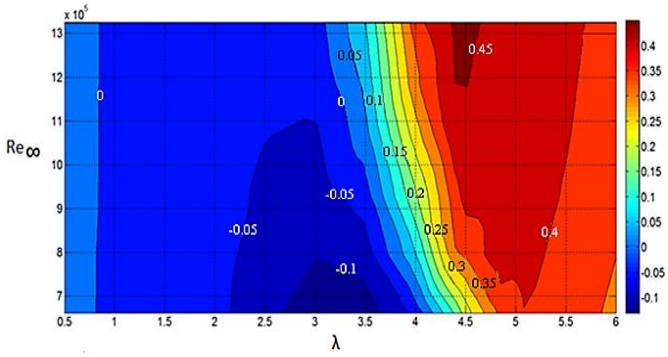

a- **Rotor Solidity □ = 0.15**

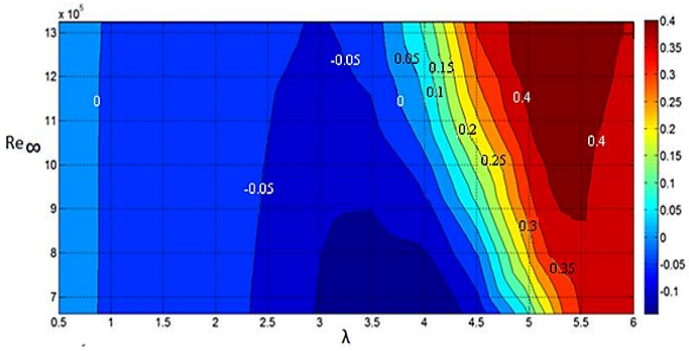

b- Rotor Solidity □ = 0.225

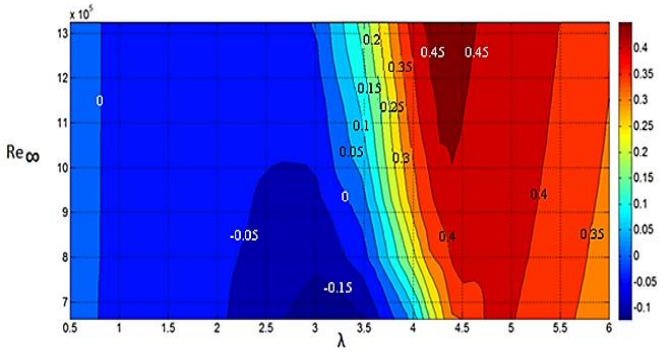

c- Rotor Solidity □ = 0.2625

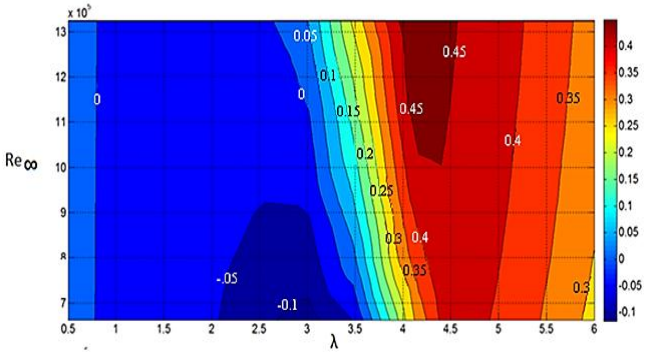

d- Rotor Solidity □ = 0.3

Fig.13 Relationship between free stream Reynolds number, tip speed ratio and power coefficient at different Rotor Solidities.

REFERENCES

[1] Paraschivoiu I., Trifu O. and Saeed F.," H-DarrieusWind Turbine with Blade Pitch Control", International Journal of Rotating Machinery, 2009.

[2] Dominy R., Lunt P., Bickerdyke A. and Dominy J.," Self-starting capability of a Darrieusturbine", Proceedings of the I MECH E part A: journal of power and energy, vol.221, pp. 111-120, 2007.

[3] Olson D. and Visser K.," Self-Starting Contra-Rotating Vertical Axis Wind Turbine for Home Heating Applications", Department of Mechanical and Aeronautical Engineering, 2009.

[4] Batista N.C., Melício R., Matias J.C.O., and CatalãoJ.P.S., "Self-Start Performance Evaluation in Darrieus-Type Vertical Axis Wind Turbines: Methodology and Computational Tool Applied to Symmetrical Airfoils", In: Proc. ICREPQ 2011, Gran Canaria, Spain (2011).

[5] Klimas P. C., " Darrieus Rotor Aerodynamics", Sandia National Laboratories, Advanced Energy Projects Division 4715, Albuquerque, NM 87185, Journal of Solar Energy Engineering, vol.104,1982.

[6] Nila I., Bogateno R. and Stere M.," Small power wind turbine (Type Darrieus)", Journal INCAS Bulletin, Vol. 4(1), pp. 135 – 142, 2012.

[7] Lobitz D. W., "Dynamic Analysis Of Darrieus Vertical Axis Wind Turbine Rotors", Sandia National Laboratories, Applied Mechanics Division, Albuquerque, New Mexico 87185.

[8] Sabaeifard,P., Razzaghi, H., and Forouzandeh, A.,"Determination of Vertical Axis Wind Turbines Optimal Configuration through CFD Simulations", International Conference on Future Environment and Energy, IACSIT Press, Singapoore, IPCBEE vol.28, 2012.

[9] Cristià. A. L, Urban Wind Turbines, MSc. Thesis, Tallin University of Technology, Estonia, 2010.

[10] Kishore. R. A, Small-scale Wind Energy Portable Turbine (SWEPT), MSc. Thesis, Virginia Polytechnic Institute and State University, Blacksburg, Virginia, 2013.

[11] Rathi. D,"Performance Prediction and Dynamic Model Analysis of Vertical Axis Wind Turbine Blades with Aerodynamically Varied Blade Pitch", MSC. Thesis, North Carolina State University, 2012.

[12] Hall. T. J," Numerical Simulation of a Cross Flow Marine Hydrokinetic Turbine", MSC. Thesis, University of Washington, 2012.

[13] Castillo. J, "Small-Scale Vertical Axis Wind Turbine Design", Bachelor's Thesis, Tampere University of Applied Sciences, 2011.

[14] Paul G. Migliore. John R. Fritschen and Richard L. Mitchell, "Darrieus Wind Turbine Airfoil Configurations", Subcontract Report No. AE-1-1045-1, Solar Energy Research Institute, 1617 cole Boulevard, Golden, Colorado 8040, 1982.

[15] Reddy. G. B.," The Darrieus Wind Turbine: An Analytic Performance Study ",MSC. Thesis, Texas Tech University, 1976.

[16] Scheurich.F, "Modelling the Aerodynamics ofVertical-Axis Wind Turbines", Ph.D. Thesis, University of Glasgow, Glasgow, UK, 2010.

[17] Manwell J. F., McGowan J. G. and Rogers A. L., "Wind Energy Explained: Theory Design and Application," second edition, John Wiley & Sons, 2009.

[18] Sheldal R. E. and Klimas P. C., "Aerodynamic Characteristics of Seven Airfoil Sections through 180 Degrees Angle of Attack for Use in Aerodynamic Analysis of Vertical Axis Wind Turbines," Sandia National Laboratories, Albuquerque, 1981.

Nomenclature

$U_{rel\ up}$	Relative velocity up wind m/s
U	Free stream velocity m/s
λ	Tip speed ratio
a_u	Induction factor up stream
φ	Azimuthal angle deg
α	Angle of attack deg
C_D	Drag coefficient
C_L	Lift coefficient
C_N	Normal force coefficient
C_t	Tangential force coefficient
C_{FT}	Thrust force coefficient
ρ	Air density kg/m^3
h	Span of blade m
c	Chord length m
R	Turbine radius m
m	Number of stream tube
a_d	Induction factor downwind
$U_{rel\ doun}$	Relative velocity downwind m/s
N	Number of blades
D	Diameter of turbine m
Ω	Turbine speed rpm